

Transition to turbulence when the Tollmien-Schlichting and bypass routes coexist

Stefan Zammert^{1,2†}, and Bruno Eckhardt^{2,3}

¹Laboratory for Aero and Hydrodynamics, Delft University of Technology,
2628 CD Delft, The Netherlands

²Fachbereich Physik, Philipps-Universität Marburg, D-35032 Marburg, Germany

³J.M. Burgerscentrum, Delft University of Technology, 2628 CD Delft, The Netherlands

(Received xx; revised xx; accepted xx)

Plane Poiseuille flow, the pressure driven flow between parallel plates, shows a route to turbulence connected with a linear instability to Tollmien-Schlichting (TS) waves, and another one, the bypass transition, that is triggered with finite amplitude perturbation. We use direct numerical simulations to explore the arrangement of the different routes to turbulence among the set of initial conditions. For plates that are a distance $2H$ apart and in a domain of width $2\pi H$ and length $2\pi H$ the subcritical instability to TS waves sets in at $Re_c = 5815$ that extends down to $Re_{TS} \approx 4884$. The bypass route becomes available above $Re_E = 459$ with the appearance of three-dimensional finite-amplitude traveling waves. The bypass transition covers a large set of finite amplitude perturbations. Below Re_c , TS appear for a tiny set of initial conditions that grows with increasing Reynolds number. Above Re_c the previously stable region becomes unstable via TS waves, but a sharp transition to the bypass route can still be identified. Both routes lead to the same turbulent in the final stage of the transition, but on different time scales. Similar phenomena can be expected in other flows where two or more routes to turbulence compete.

1. Introduction

The application of ideas from dynamical systems theory to the turbulence transition in flows without linear instability of the laminar profile, such as pipe flow or plane Couette flow have provided a framework in which many of the observed phenomena can be rationalized. This includes the sensitive dependence on initial conditions (Darbyshire & Mullin 1995; Schmiegel & Eckhardt 1997), the appearance of exact coherent states around which the turbulent state can form (Nagata 1990; Clever & Busse 1997; Waleffe 1998; Faisst & Eckhardt 2003; Wedin & Kerswell 2004; Gibson *et al.* 2009), the transience of the turbulent state (Hof *et al.* 2006; Schneider & Eckhardt 2008; Vollmer *et al.* 2009; Kreilos & Eckhardt 2012), or the complex spatio-temporal dynamics in large systems (Bottin *et al.* 1998; Manneville 2009; Barkley & Tuckerman 2005; Moxey & Barkley 2010; Avila *et al.* 2011). Methods to identify the critical thresholds that have to be crossed before the turbulent state can be reached have been developed (Willis & Kerswell 2007; Cherubini *et al.* 2011b) and the bifurcation and manifold structures that explains this behavior in the state space of the system have been identified (Halcrow *et al.* 2009). Extensions to open external flows, like asymptotic suction boundary layers (Kreilos *et al.* 2013; Khapko

† Email address for correspondence: Stefan.Zammert@gmail.com

et al. 2013, 2014, 2016) and developing boundary layers (Cherubini *et al.* 2011*a*; Duguet *et al.* 2012; Wedin *et al.* 2014) have been proposed.

Plane Poiseuille flow (PPF), the pressure driven flow between parallel plates, shows a transition to turbulence near a Reynolds number of about 1000 (Carlson *et al.* 1982; Lemoult *et al.* 2012; Tuckerman *et al.* 2014). In the subcritical range the flow shows much of the transition phenomenology observed in other subcritical flows, such as plane Couette flow or pipe flow, but it also has a linear instability of the laminar profile at a Reynolds number of 5772 (Orszag 1971). This raises the question about the relation between the transition via an instability to the formation of Tollmien-Schlichting (TS) waves and the transition triggered by large amplitude perturbations that bypass the linear instability (henceforth referred to as the "bypass" transition) (Schmid & Henningson 2001). For instance, one could imagine that the exact coherent structures related to the bypass transition are connected to the TS waves in some kind of subcritical bifurcation. However, the flow structures are very different, with the exact coherent structures being dominated by downstream vortices (Zammert & Eckhardt 2014, 2015), and the TS waves dominated by spanwise vortices.

In order to explore the arrangement of the different transition pathways we will use direct numerical simulations to map out the regions of initial conditions that follow one or the other path. Such explorations of the state space of a flow have been useful in the identification of the sensitive dependence on initial conditions for the transition (Schmiegel & Eckhardt 1997; Faisst & Eckhardt 2004), and in the exploration of the bifurcations (Kreilos & Eckhardt 2012; Kreilos *et al.* 2014).

We start with a description of the system and the bifurcations of the relevant coherent states in section 2. Afterwards, in section 3 we describe the exploration of the state space of the system. Conclusions are summarized in section 4.

2. Plane Poiseuille flow and its coherent structures

To fix the geometry, let x , y , and z be the downstream, normal and spanwise directions, and let the flow be bounded by parallel plates at $y = \pm H$. The flow is driven by a pressure gradient, giving a parabolic profile for the laminar flow. Dimensionless units are formed with the height H and the center line velocity U_0 so that the unit of time is H/U_0 and the Reynolds number becomes $Re = U_0 H/\nu$, with ν the fluid viscosity. In these units the laminar profile becomes $\vec{u}_0 = (1 - y^2)\vec{e}_x$. The equations of motion, the incompressible Navier-Stokes equations, are solved using *Channelflow* (Gibson 2012), with a spatial resolution of $N_x = N_z = 32$ and $N_y = 65$ for a domain of length 2π and width 2π and at fixed mass flux. The chosen resolution is sufficient to resolve the exact solutions and the transition process but underresolved in the turbulent case. In the studied domain, the linear instability occurs at $Re_c = 5815$, slightly higher than the value found by Orszag (1971) on account of the slightly different domain size.

The full velocity field $\vec{U} = \vec{u}_0 + \vec{u}$ can be written as a sum of the laminar flow \vec{u}_0 and deviations $\vec{u} = (u, v, w)$. In the following we always mean \vec{u} when we refer to the velocity field. Tollmien-Schlichting (TS) waves are travelling waves formed by spanwise vortices. They appear in a subcritical bifurcation that extends down to $Re \approx 2610$ for a streamwise wavenumber of 1.36. The TS wave is independent of spanwise position z and consists of two spanwise vortices, as shown in figure 1(a).

The Reynolds number range over which the transition to TS waves is subcritical depends on the domain size. For our domain (streamwise wave number of 1.0) the turning point is at $Re \approx 4685$. A bifurcation diagram of this exact solution, referred to as TW_{TS} in the remainder of the paper, is shown in figure 2(a). The ordinate in the bifurcation

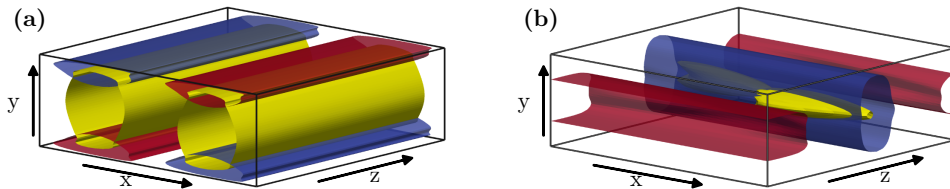


FIGURE 1. The exact coherent states for the transition to turbulence in plane Poiseuille flow. (a) Visualization of the Tollmien-Schlichting wave TW_{TS} . The yellow surface indicates values of $0.3Q_{max}$ for the Q-vortex criterion. The red and the blue surface correspond to $u = \pm 0.1$, respectively. (b) Visualization of the edge state TW_E for the bypass transition. As before, the yellow surface indicates values of $0.3Q_{max}$ for the Q-vortex criterion. The levels for the red and blue surfaces are now $u = 0.008$ and $u = -0.014$, respectively.

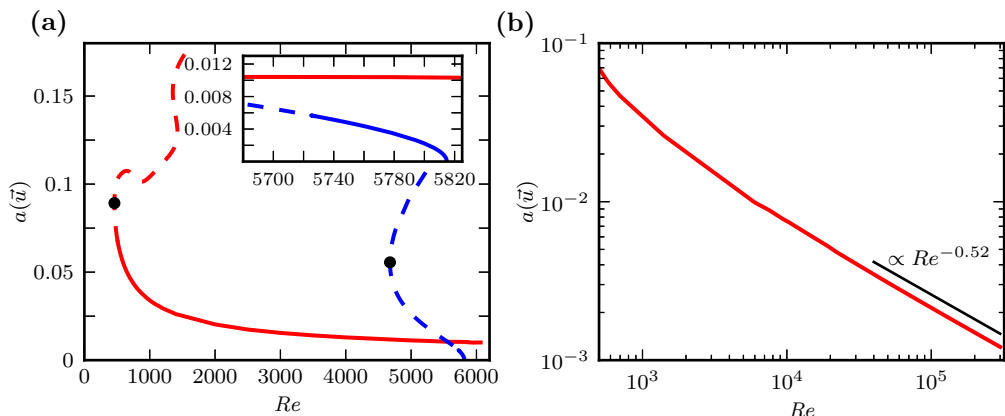


FIGURE 2. The bifurcation diagrams for TW_E (red) and TW_{TS} (blue) are shown in panel (a). A solid line is used if the travelling wave has just one unstable eigenvalue, while a dashed line is used when the wave has further unstable eigenvalues. The inset zooms in on the region where both waves have only one unstable eigenvalues. The bifurcation points of the waves are marked with black dots. In panel (b) the amplitude $a(\vec{u})$ of TW_E is shown in a double-logarithmic plot, together with a powerlaw decay like $Re^{-0.52}$ for large Re .

diagram is the amplitude of the flow field

$$a(\vec{u}) = \|\vec{u}\| = \sqrt{\frac{1}{L_x L_y L_z} \int \vec{u}^2 dx dy dz}. \quad (2.1)$$

A study of the stability of the state in the full three-dimensional space shows that this lower branch state has only one unstable direction in the used computational domain for $5727 < Re < 5815 = Re_c$. Thus, for these Reynolds numbers the state is an *edge state* whose stable manifold can divide the state space in two parts (Skufca *et al.* 2006). For lower Re , there are secondary bifurcations that add more unstable directions to the state. Specifically, near the turning point at $Re = 4690$, the lower branch has acquired about 350 unstable directions. Because of the high critical Reynolds numbers this state cannot explain the transition to turbulence observed in experiments at Reynolds numbers around 1000 (Carlson *et al.* 1982; Nishioka & Asai 1985; Lemoult *et al.* 2012, 2013) or even lower (Sano & Tamai 2016).

The states that are relevant to the bypass transition can be found using the method of edge tracking (Toh & Itano 2003; Schneider *et al.* 2007, 2008). Starting from an arbitrary turbulent initial condition, trajectories in the laminar-turbulent-boundary that

are followed with the edge-tracking algorithm converge to a travelling wave (Zammert & Eckhardt 2014) which we referred to as TW_E in the following. The visualization in figure 1(b) shows that this state has a strong narrow upstream streak, a weaker but more extended downstream streak and streamwise vortices. Moreover, TW_E has a wall-normal reflection symmetry

$$s_y : [u, v, w](x, y, z) = [u, -v, w](x, -y, z), \quad (2.2)$$

a shift-and-reflect symmetry

$$s_z \tau_x : [u, v, w](x, y, z) = [u, v, -w](x + 0.5 \cdot L_x, y, -z), \quad (2.3)$$

and exists for a wide range in Reynolds numbers. It is created in a saddle-node bifurcation near $Re \approx 459$ (see the bifurcation diagram in figure 2(a)); for other combinations of spanwise and streamwise wavelengths the state appears at a even lower Reynolds numbers of 319 (Zammert & Eckhardt 2017). The corresponding lower branch state can be continued to Reynolds numbers far above $3 \cdot 10^5$, and its amplitude decreases with increasing Reynolds number as shown in figure 2(b). A fit to the amplitude for large Reynolds numbers gives a scaling like $Re^{-0.52}$, similar to that of the solution embedded in the edge of plane Couette flow (Itano *et al.* 2013). A stability analysis of the lower branch of TW_E shows that the travelling wave has one unstable eigenvalue for $510 < Re < 5850$. Therefore, TW_E is a second travelling wave with a stable manifold that can divide the state space into two disconnected parts. How the two edge states interact and divide up the state space will be discussed in section 3.

At $Re = 510$ the lower branch undergoes a supercritical pitchfork bifurcation that breaks the s_y symmetry and adds a second unstable eigenvalues for $Re < 510$. The upper branch of the travelling wave has three unstable eigenvalues for $Re < 1000$. Investigation of different systems which show subcritical turbulence revealed that bifurcations of exact solutions connected to the edge state of the system lead to the formation of a chaotic saddle that shows transient turbulence with exponential distributed lifetimes (Kreilos & Eckhardt 2012; Avila *et al.* 2013). In the present systems the formation of chaotic saddle cannot be studied in detail since it takes place in an unstable subspace. However, previous investigations in a symmetry restricted system did show that the states follow such a sequence of bifurcations to the formation of a chaotic saddle (Zammert & Eckhardt 2015, 2017), so that we expect that also the states in the unstable subspace follow this phenomenology.

The two travelling waves described above are clearly related to the two different transition mechanism that exist in the flow. For Reynolds numbers below the onset of TS waves (here: $Re_c = 5815$), initial conditions that start close to TW_E in the state space will either decay or become turbulent without showing any approach to a TS wave: they will follow the bypass transition to turbulence. Initial condition that start close to TW_{TS} can also either decay or swing up to turbulence, but they will first form TS waves. Above Re_c all initial conditions will show a transition to turbulence, but it will still be possible to distinguish whether they follow the bypass or TS route to turbulence, as we will see.

3. State space structure

In order to explore the arrangement of the different routes to turbulence in the space of initial conditions we pick initial conditions and integrate them until the flow either becomes turbulent or until it returns to the laminar profile. The initial conditions are taken in a two-dimensional slice of the high-dimensional space, spanned by two flow fields

\vec{u}_1 and \vec{u}_2 . The choice of the flow fields allows to explore different cross sections of state space. For the most part, we will use \vec{u}_1 and \vec{u}_2 to be the travelling waves TW_E and TW_{TS} , so that both states are part of the cross section. The initial conditions are then parametrized by a mixing parameter α and an amplitude A , i.e.,

$$\vec{u}(\alpha, A) = A \frac{(1 - \alpha)\vec{u}_1 + \alpha\vec{u}_2}{\|(1 - \alpha)\vec{u}_1 + \alpha\vec{u}_2\|}. \quad (3.1)$$

For $\alpha = 0$ one explores the state space along velocity field \vec{u}_1 and for $\alpha = 1$ along velocity field \vec{u}_2 . If the upper and lower branch of TW_E are used to create such a slice, one recognizes that the turbulence in PPF appears in similar chaotic bubbles as in plane Couette (Kreilos & Eckhardt 2012; Zammert & Eckhardt 2015).

Lower branch states are relevant for the transition to turbulence, so begin by exploring the slice spanned by the lower branches of TW_E and TW_{TS} . We assign to each initial condition the time it takes to become turbulent, with an upper cut-off for initial conditions that either take longer or that never become turbulent because they return to the laminar profile. Color coded transition-time plots are shown in figure ??(a) - (e) for different Reynolds numbers below Re_c . The boundary between initial conditions that relaminarize and those that become turbulent stands out clearly. They are formed by the stable manifold of the states and their crossings with the cross section. Parts of the stable manifold are indicated by the dashed white lines for better visibility. The part of the laminar-turbulent boundary connected with TW_E can be distinguished from that connected to TW_{TS} by the huge differences in transition times: for TW_{TS} transition times are significantly longer and even exceed $2 \cdot 10^4$ time units. The interaction between the two domains is rather intricate. For Reynolds number 5780, shown in figure ??(d), it seems that the borders do not cross but rather wind around each other in a spiral shape down to very small scales. Although the wave TW_{TS} has still only one unstable eigenvalues, the size of the structure that is directly connected to TW_{TS} shrinks with decreasing Re and is not visible in these kind of projection for $Re < 5727$ where TW_{TS} has more than one unstable eigenvalue.

In figure 4 the evolution of the amplitude for different initial conditions marked in figure ??(d) is shown. The green and blue lines are typical representatives of the slow TS transition. Starting with a three dimensional initial condition, their amplitude decays and the two-dimensional TS wave TW_{TS} , whose amplitude is marked by the black line, is approached. Afterwards, they depart from TW_{TS} again, which is a slow process because of the small growth rate. Ultimately, the transition is caused by secondary instabilities of the TS waves (Herbert 1988).

The solid yellow line in figure 4 is an initial condition that undergoes bypass transition. It quickly swings up to higher amplitudes and does not approach the TS wave on its way to turbulence. The dashed yellow line is of an intermediate type. It takes a long time to become turbulent but it does not come very close to the TS wave. The relation between time-evolution, transient amplification, and final state is complicated and non-intuitive. For instance, the dashed red and green trajectories share a transients increase near $t \approx 4000$, but differ in their final state: the red curve, with the higher maximum, eventually returns to the laminar profile, but the green curve, with the smaller maximum, approaches the TS level and eventually becomes turbulent following the TS route. Similarly, the red, blue and green continuous lines start with high amplitude slightly below the threshold for the bypass route. They all decay, but while the red initial conditions ends up on the decaying side of the TS wave, the green and blue one eventually become turbulent via the TS route.

For plane Couette flow it was found that a small chaotic saddle can appear inside of

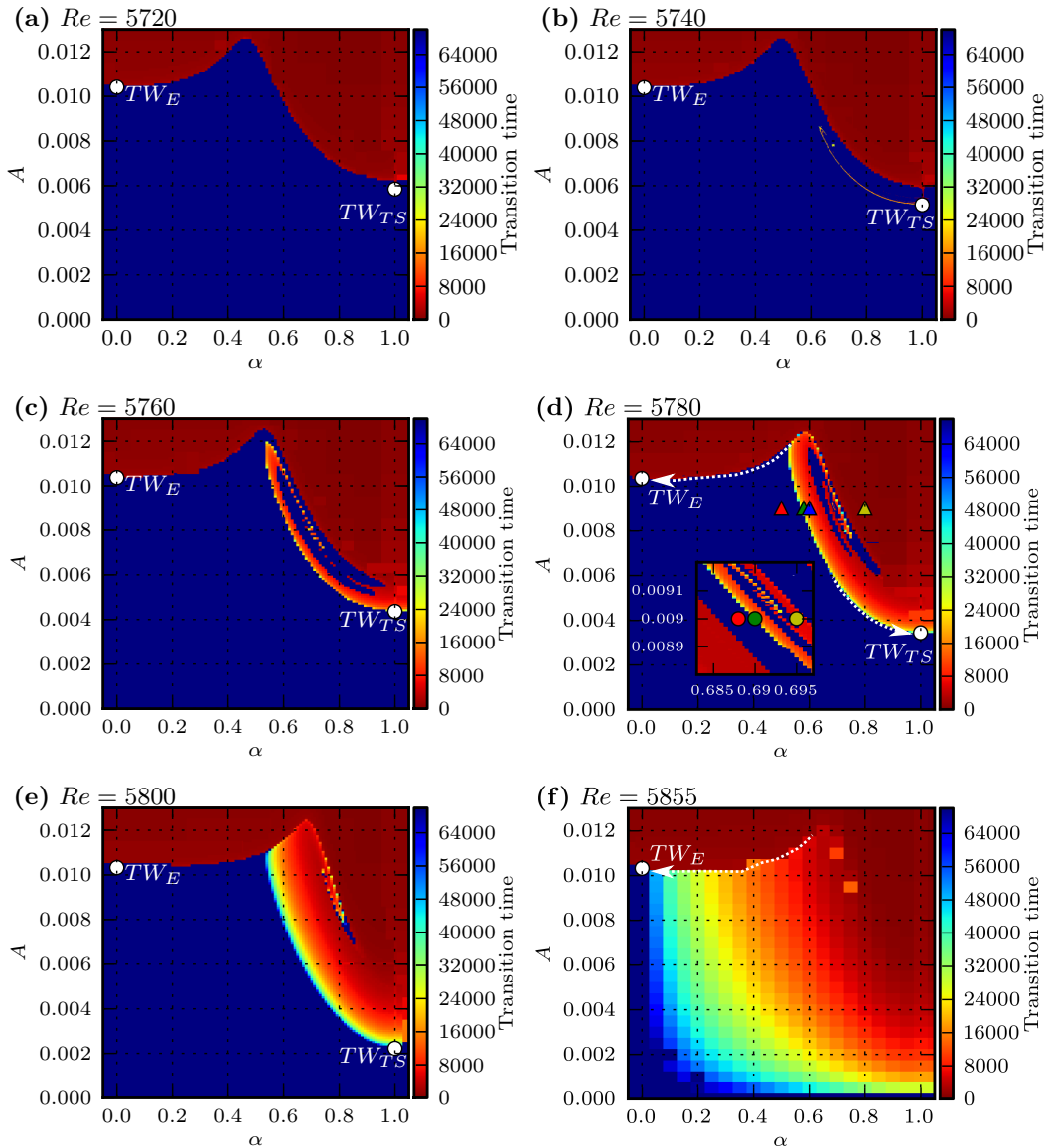


FIGURE 3. Two-dimensional slices of the state space for various Reynolds numbers. In panel (a-e), where $Re < Re_c = 5815$, the parameter α interpolates between the flow fields of both traveling waves, and both are indicated by white dots in the figures. In panel (f), where $Re > Re_c$ the plane is spanned by the flow field of TW_E and by the unstable TS-mode of the laminar state. In all panels the color indicates the time it takes to reach the turbulent states, up to a maximum integration time of 70000 time units. Accordingly, initial conditions that do not become turbulent or return to the laminar state are indicated by dark blue. The dashed lines in panels (d) and (f) indicate the stable manifolds of the corresponding fixed points. The colored triangles and dots in panel (d) mark initial conditions whose time evolution is shown in figure 4.

existing larger ones (Kreilos *et al.* 2014). There, trajectories that escape from the inner saddle are still captured by the outer one. The appearance of TS transition in PPF follows a comparable mechanism. With increasing Reynolds number the chaotic saddle of subcritical bypass turbulence is surrounded by the stable manifold of the TS wave

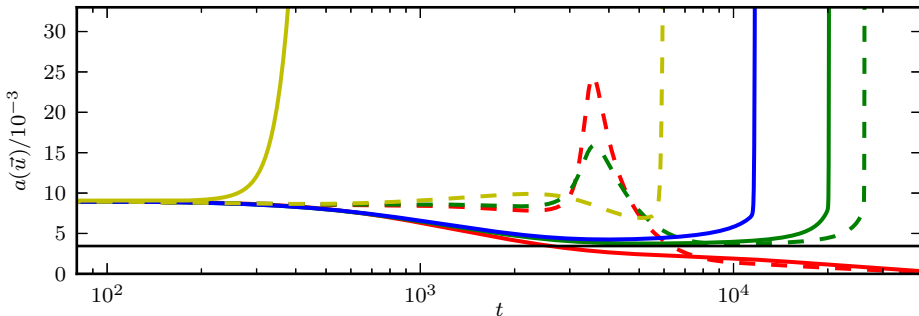


FIGURE 4. Time evolution of the velocity amplitude $a(\bar{u})$ for the initial conditions marked in figure ??(d) for $Re = 5780$. The initial conditions for the trajectories drawn with solid and dashed lines are marked in figure ??(b) with triangles and circles, respectively. The black line indicates the amplitude of the lower branch of the TS state TW_{TS} at $Re = 5780$. Some of the initial conditions that miss the bypass transition become turbulent nevertheless because they are captured by the TS instability (e.g. the full blue, and both green lines).

that above $Re = 5727$ can separate two parts of the state space and therefore prevent trajectories in the interior from becoming laminar.

With increasing Reynolds number the number of initial conditions becoming turbulent increases. Finally, for $Re > Re_c$ no initial conditions that return to the laminar state exist anymore. Nevertheless, also in this supercritical regime a sudden change in the type of transition can be identified: when the amplitude increases and crosses the stable manifold of TW_E , the transition time drops dramatically and turbulence is reached via the bypass route. In the state space visualization for $Re = 5855$ that is shown in figure ??(c), these change of the transition type presents itself in the rapid drop of the transition time with increasing a for α values between 0 and 0.6.

In the supercritical range the stable manifold of the bypass edge state TW_E separates initial conditions undergoing the quick bypass transition from initial conditions that become turbulent by TS transition. The state space picture at a higher Reynolds number of 6000 looks qualitatively similar to the one shown in figure ??(c), including the switch from TS to bypass transition when the stable manifold of TW_E is crossed.

4. Conclusions

We have explored the coexistence of two types of transition in subcritical plane Poiseuille flow connected with the existence of states dominated by streamwise and spanwise vortices (bypass and TS transition). Probing the state space by scanning initial conditions in two-dimensional cross sections gave information on the sets of initial conditions that follow one or the other route to turbulence. The results show that the transition via TS waves initially occupies a tiny region of state space. As this region expands it approaches the bypass-dominated regions, but a boundary between the two remains visible because of the very different times needed to reach turbulence. This extends to the parameter range where the laminar profile is unstable to the formation of TS waves.

The results shown here are obtained for small domains, where the extensive numerical computations for very many initial conditions are feasible. For larger domains, the corresponding exact coherent structures are localized, as shown by Jiménez (1990) and Mellibovsky & Meseguer (2015) for TS waves and by Zammert & Eckhardt (2014) for

the bypass transition. Since the bifurcation diagrams for the localized states are similar to that of the extended states, we anticipate a similar phenomenology also for localized perturbations in spatially extended states.

The methods presented here can also be used to explore the relation between bypass transition and TS waves in boundary layers (Duguet *et al.* 2012; Kreilos *et al.* 2016). More generally, they can be applied to any kind of transition where two different paths compete: examples include shear driven or convection driven instabilities in thermal convection (Clever & Busse 1992; Zammert *et al.* 2016), the interaction between transitions driven by different symmetries (Faisst & Eckhardt 2003; Wedin & Kerswell 2004; Schneider *et al.* 2008), or the interaction between the established subcritical scenario and the recently discovered linear instability in Taylor-Couette flow with rotating outer cylinder (Deguchi 2017).

This work was supported in part by the German Research Foundation (DFG) within Forschergruppe 1182.

REFERENCES

- AVILA, K., MOXEY, D., DE LOZAR, A., AVILA, M., BARKLEY, D. & HOF, B. 2011 The onset of turbulence in pipe flow. *Science* **333** (6039), 192–6.
- AVILA, M., MELLIBOVSKY, F., ROLAND, N. & HOF, B. 2013 Streamwise-localized solutions at the onset of turbulence in pipe flow. *Phys. Rev. Lett.* **110**, 224502.
- BARKLEY, D. & TUCKERMAN, L. 2005 Computational Study of Turbulent Laminar Patterns in Couette Flow. *Phys. Rev. Lett.* **94**, 014502.
- BOTTIN, S., DAVIAUD, F., MANNEVILLE, P. & DAUCHOT, O. 1998 Discontinuous transition to spatiotemporal intermittency in plane Couette flow. *Europhys. Lett.* **43** (2), 171–176.
- CARLSON, D. R., WIDNALL, S. E. & PEETERS, M. F. 1982 A flow-visualization study of transition in plane Poiseuille flow. *J. Fluid Mech.* **121**, 487–505.
- CHERUBINI, S., DE PALMA, P., ROBINET, J.-C. & BOTTARO, A. 2011a Edge states in a boundary layer. *Phys. Fluids* **23** (5), 051705.
- CHERUBINI, S., DE PALMA, P., ROBINET, J.-C. & BOTTARO, A. 2011b The minimal seed of turbulent transition in the boundary layer. *J. Fluid Mech.* **689**, 221–253.
- CLEVER, R. M. & BUSSE, F. H. 1992 Three-dimensional convection in a horizontal fluid layer subjected to a constant shear. *J. Fluid Mech.* **234**, 511–527.
- CLEVER, R. M. & BUSSE, F. H. 1997 Tertiary and quaternary solutions for plane Couette flow. *J. Fluid Mech.* **344**, 137–153.
- DARBYSHIRE, A. G. & MULLIN, T. 1995 Transition to turbulence in constant-mass-flux pipe flow. *J. Fluid Mech.* **289**, 83–114.
- DEGUCHI, KENGO 2017 Linear instability in Rayleigh-stable Taylor-Couette flow. *Phys. Rev. E* p. in press.
- DUGUET, Y., SCHLATTER, P., HENNINGSON, D. S. & ECKHARDT, B. 2012 Self-sustained localized structures in a boundary-layer flow. *Phys. Rev. Lett.* **108**, 044501.
- FAISST, H. & ECKHARDT, B. 2003 Traveling waves in pipe flow. *Phys. Rev. Lett.* **91**, 224502.
- FAISST, H. & ECKHARDT, B. 2004 Sensitive dependence on initial conditions in transition to turbulence in pipe flow. *J. Fluid Mech.* **504**, 343–352.
- GIBSON, J. F. 2012 Channelflow: a spectral Navier-Stokes simulator in C++. *Tech. Rep.*. U. New Hampshire.
- GIBSON, J. F., HALCROW, J. & CVITANOVIĆ, P. 2009 Equilibrium and travelling-wave solutions of plane Couette flow. *J. Fluid Mech.* **638**, 243–266.
- HALCROW, J., GIBSON, J. F., CVITANOVIĆ, P. & VISWANATH, D. 2009 Heteroclinic connections in plane Couette flow. *J. Fluid Mech.* **621**, 365–376.
- HERBERT, T. 1988 Secondary instability of boundary layers. *Annu. Rev. Fluid Mech.* **20**, 487–526.
- HOF, B., WESTERWEEL, J., SCHNEIDER, T. M. & ECKHARDT, B. 2006 Finite lifetime of turbulence in shear flows. *Nature* **443** (7107), 59–62.

- ITANO, T., AKINAGA, T., GENERALIS, S. C. & SUGIHARA-SEKI, M. 2013 Transition of Planar Couette Flow at Infinite Reynolds Numbers. *Phys. Rev. Lett.* **111**, 184502.
- JIMÉNEZ, J. 1990 Transition to turbulence in two-dimensional Poiseuille flow. *J. Fluid Mech.* **218**, 265–297.
- KHAPKO, T., DUGUET, Y., KREILOS, T., SCHLATTER, P., ECKHARDT, B. & HENNINGSON, D. S. 2014 Complexity of localised coherent structures in a boundary-layer flow. *Eur. Phys. J. E* **37** (32), 1–12.
- KHAPKO, T., KREILOS, T., SCHLATTER, P., DUGUET, Y., ECKHARDT, B. & HENNINGSON, D. S. 2013 Localized edge states in the asymptotic suction boundary layer. *J. Fluid Mech.* **717**, R6.
- KHAPKO, TARAS, KREILOS, TOBIAS, SCHLATTER, PHILIPP, DUGUET, YOHANN, ECKHARDT, BRUNO & HENNINGSON, DAN S. 2016 Edge states as mediators of bypass transition in boundary-layer flows. *J. Fluid Mech.* **801**, R2, arXiv: 1605.03002.
- KREILOS, T. & ECKHARDT, B. 2012 Periodic orbits near onset of chaos in plane Couette flow. *Chaos* **22** (4), 047505.
- KREILOS, TOBIAS, ECKHARDT, BRUNO & SCHNEIDER, TOBIAS M. 2014 Increasing Lifetimes and the Growing Saddles of Shear Flow Turbulence. *Phys. Rev. Lett.* **112**, 044503.
- KREILOS, T., KHAPKO, T., SCHLATTER, P., DUGUET, Y.N, HENNINGSON, D. S. & ECKHARDT, BRUNO 2016 Bypass transition and spot nucleation in boundary layers. *Phys. Rev. Fluids* **1**, 043602, arXiv: 1604.07235.
- KREILOS, T., VEBLE, G., SCHNEIDER, T. M. & ECKHARDT, B. 2013 Edge states for the turbulence transition in the asymptotic suction boundary layer. *J. Fluid Mech.* **726**, 100–122.
- LEMOULT, G., AIDER, J.-L. & WESFREID, J. E. 2012 Experimental scaling law for the subcritical transition to turbulence in plane Poiseuille flow. *Phys. Rev. E* **85** (2), 025303(R).
- LEMOULT, G., AIDER, J.-L. & WESFREID, J. E. 2013 Turbulent spots in a channel: large-scale flow and self-sustainability. *J. Fluid Mech.* **731**, R1.
- MANNEVILLE, P. 2009 Spatiotemporal perspective on the decay of turbulence in wall-bounded flows. *Phys. Rev. E* **79**, 025301.
- MELLIBOVSKY, F. & MESEGUER, A. 2015 A mechanism for streamwise localisation of nonlinear waves in shear flows. *J. Fluid Mech.* **779**, R1.
- MOXEY, D. & BARKLEY, D. 2010 Distinct large-scale turbulent-laminar states in transitional pipe flow. *Proc. Natl. Acad. Sci. U. S. A.* **107** (18), 8091–8096.
- NAGATA, M 1990 Three-dimensional finite-amplitude solutions in plane Couette flow: bifurcation from infinity. *J. Fluid Mech* **217**, 519–527.
- NISHIOKA, M. & ASAI, M. 1985 Some observations of the subcritical transition in plane Poiseuille flow. *J. Fluid Mech.* **150**, 441–450.
- ORSZAG, S. A. 1971 Accurate solution of the Orr-Sommerfeld stability equation. *J. Fluid Mech.* **50**, 689–703.
- SANO, M. & TAMAI, K. 2016 A Universal Transition to Turbulence in Channel Flow. *Nat. Phys.* **12**, 249–253.
- SCHMID, P & HENNINGSON, DAN S 2001 *Stability and transition in shear flow*. Springer Berlin / Heidelberg.
- SCHMIEGEL, A. & ECKHARDT, B. 1997 Fractal Stability Border in Plane Couette Flow. *Phys. Rev. Lett.* **79**, 5250.
- SCHNEIDER, T. M. & ECKHARDT, B. 2008 Lifetime statistics in transitional pipe flow. *Phys. Rev. E* **78**, 046310.
- SCHNEIDER, T. M., ECKHARDT, B. & YORKE, J. 2007 Turbulence transition and the edge of chaos in pipe flow. *Phys. Rev. Lett.* **99**, 034502.
- SCHNEIDER, T. M., GIBSON, J. F., LAGHA, M., DE LILLO, F. & ECKHARDT, B. 2008 Laminar-turbulent boundary in plane Couette flow. *Phys. Rev. E* **78**, 037301.
- SKUFGA, J., YORKE, J. A. & ECKHARDT, B. 2006 Edge of chaos in a parallel shear flow. *Phys. Rev. Lett.* **96**, 174101.
- TOH, S. & ITANO, T. 2003 A periodic-like solution in channel flow. *J. Fluid Mech.* **481**, 67–76.
- TUCKERMAN, L. S., KREILOS, T., SCHROBSDORFF, H, SCHNEIDER, T. M. & GIBSON, J. F. 2014 Turbulent-laminar patterns in plane Poiseuille flow. *Phys. Fluids* **26**, 114103.

- VOLLMER, J., SCHNEIDER, T. M. & ECKHARDT, B. 2009 Basin boundary, edge of chaos and edge state in a two-dimensional model. *New J. Phys.* **11**, 013040.
- WALEFFE, F. 1998 Three-Dimensional Coherent States in Plane Shear Flows. *Phys. Rev. Lett.* **81** (19), 4140.
- WEDIN, H., BOTTARO, A., HANIFI, A & ZAMPOGNA, G. 2014 Unstable flow structures in the Blasius boundary layer. *Eur. Phys. J. E* **37** (34), 1–20.
- WEDIN, H. & KERSWELL, R. R. 2004 Exact coherent structures in pipe flow: travelling wave solutions. *J. Fluid Mech.* **508**, 333–371.
- WILLIS, A. & KERSWELL, R. R. 2007 Critical Behavior in the Relaminarization of Localized Turbulence in Pipe Flow. *Phys. Rev. Lett.* **98** (1), 014501.
- ZAMMERT, S & ECKHARDT, B. 2014 Streamwise and doubly-localised periodic orbits in plane Poiseuille flow. *J. Fluid Mech.* **761**, 348–359.
- ZAMMERT, S. & ECKHARDT, B. 2015 Crisis bifurcations in plane Poiseuille flow. *Phys. Rev. E* **91**, 041003(R).
- ZAMMERT, S. & ECKHARDT, B. 2017 Harbingers and latecomers - The order of appearance of exact coherent structures in plane Poiseuille flow. *J. Turbul.* **18** (2), 103–114.
- ZAMMERT, S. & ECKHARDT, B. 2015 Bypass transition and subcritical turbulence in plane Poiseuille flow. *Proceedings of TSFP-9*, www.tsfp-conference.org, arXiv:1506.04370.
- ZAMMERT, S., FISCHER, N. & ECKHARDT, B. 2016 Transition in the asymptotic suction boundary layer over a heated plate. *J. Fluid Mech.* **803**, 175–199.